1-15-2018

Modeling Multicomponent Fuel Droplet Vaporization with Finite Liquid Diffusivity Using Coupled Algebraic-Dqmom with Delumping

Alanna Y. Cooney
Marquette University

Simcha L. Singer
Marquette University, simcha.singer@marquette.edu

Accepted version. *Fuel*, Vol. 212 (January 15, 2018): 554-565. DOI.

Modeling multicomponent fuel droplet vaporization with finite liquid diffusivity using Coupled Algebraic-DQMoM with delumping

Alanna Y. Cooney
Department of Mechanical Engineering, Marquette University, Milwaukee, WI
Simcha L. Singer
Department of Mechanical Engineering, Marquette University, Milwaukee, WI

Abstract

Multicomponent fuel droplet vaporization models for use in combustion CFD codes often prioritize computational efficiency over model complexity. This leads to oversimplifying assumptions such as single component droplets or infinite liquid diffusivity. The previously developed Direct Quadrature Method of Moments (DQMoM) with delumping model demonstrated a computationally efficient and

accurate approach to solve for every discrete species in a well-mixed vaporizing multicomponent droplet. To expand the method to less restrictive cases, a new solution technique is presented called the Coupled Algebraic-Direct Quadrature Method of Moments (CA-DQMoM). In contrast to previous moment methods for droplet vaporization, CA-DQMoM solves for the evolution of two liquid distributions by coupling a monovariate, homogeneous DQMoM approach with additional algebraic moment equations, allowing for a more complex droplet vaporization model with finite rates of liquid diffusion to be solved with computational efficiency. To further decrease computational expense, an approximation that employs the same nodes for both distributions can be used in certain cases. Finally, a delumping technique is adapted to the finite diffusivity model to reconstruct discrete species information at minimal computational cost. The model is proven to be accurate relative to a full discrete component model for both a kerosene droplet comprised of 36 species and a multicomponent droplet of 200 species while maintaining the computational efficiency of continuous thermodynamics models. The combined accuracy and computational efficiency demonstrated by the CA-DQMoM with delumping model for a multicomponent fuel droplet with finite liquid diffusivity makes it ideal for incorporation into CFD models for complex combustion process.

Keywords

Multicomponent droplet vaporization, Continuous thermodynamics, Coupled Algebraic-Direct Quadrature Method of Moments, Delumping, Liquid diffusion, Parabolic

Nomenclature

A	group of variables
B_M	Spalding mass transfer number
B_T	Spalding heat transfer number
C	molar concentration, group of variables
c_p	specific heat capacity
D	diffusion coefficient
E	group of variables
f	function
G	group of variables
I	distribution variable
k	thermal conductivity
l_v	latent heat of vaporization
m	moment
N	number of CA-DQMoM nodes
Nu	Nusselt number
n	number of discrete species
$\dot{n}$	molar flow rate
P	pressure
r	radial coordinate
R	radius of droplet
R_f	radius of gas film
S	source term in CTM species equation

$\bar{S}$ source term in moment transformed species equation
Sh Sherwood number
T temperature
$\bar{T}$ volume averaged temperature
t time coordinate
u integrating factor
w CA-DQMoM weight
x mole fraction
$\bar{x}$ volume averaged mole fraction
δ delta function

Superscripts

$*$ modified (Sherwood number, Nusselt number)
i discrete species index
j CA-DQMoM node index
k moment order index
tot total (for all species)

Subscripts

c evaluated at the droplet center
g gas
i discrete species index
j CA-DQMoM node index
k moment order index
l liquid
nb normal boiling
s evaluated at droplet surface
sat saturation
v vapor
∞ at far-field boundary

1. Introduction

Accurate knowledge of the vapor molar flow rates of discrete species during the vaporization of multicomponent liquid fuel droplets is important when modeling combustion processes using computational fluid dynamics (CFD). Computational efficiency is an important factor when developing these models, leading to the need for a balance between computational expense and model accuracy. Solution methods previously developed for multicomponent droplet vaporization include discrete component models (DCM),[1,2,3] quasi-discrete models,[4,5] and continuous thermodynamic models (CTM).[6,7,8,9,10,11,12,13,14] DCM approaches solve equations for each discrete species comprising a multicomponent droplet and are therefore accurate but computationally expensive. Alternatively, CTM approaches characterize the multicomponent mixture composition as a continuous function of a distribution variable, typically normal boiling temperature or molecular weight. While CTM approaches improve computational efficiency, they cannot provide information on the vaporization or condensation rates of discrete droplet species.

DCMs for multicomponent droplet vaporization previously developed include the partial differential equation (PDE) model by Torres et al.,[1] the infinite diffusivity model developed by Ra and Reitz,[2] and the combined transient to quasi-steady parabolic model presented by Brereton.[3] Although the models of[2] and[3] improve upon the computational efficiency of[1] by making simplifying assumptions, these DCMs still become computationally impractical for droplets with a large number of components.

CTM approaches have therefore been developed to increase computational efficiency. Well-mixed, multi-component droplet vaporization was modeled by Tamim and Hallet6 and Hallet[7] by assuming the probability density function used to represent the droplet composition was a gamma function. Wang and Lee[8] also utilized a gamma function in their model which accounted for finite rates of liquid diffusion. To increase flexibility in the gamma function model, Harstad et al. developed a double gamma function PDF approach to more accurately account for condensation on the droplet.[9,10] Laurent et al. demonstrated that there are limitations to assuming the shape of the PDF is a gamma function[11] and developed a new approach for modeling multicomponent droplet vaporization by applying Lage's version of the Quadrature Method of Moments (QMoM)[15] to a well-mixed droplet.[11,12] Noting the numerical complications which can arise utilizing QMoM, Bruyat et al. used the Direct Quadrature Method of Moments (DQMoM) as an alternative method for modeling well-mixed droplet vaporization.[13] For simplicity, CTM approaches most often utilize molar conservation equations,[16] as opposed to the classically defined mass based equations, which leads to different, but equally acceptable, assumptions for the constant gas phase properties.[17]

DQMoM was originally developed for various monovariate and multivariate population balance equations (PBE) for both spatially homogeneous and inhomogeneous conditions.[18] By assuming infinite liquid diffusivity, the well-mixed droplet model[13] eliminates spatial dependence and is therefore solved using a monovariate, spatially homogeneous DQMoM approach which solves a set of ODEs for the DQMoM weights and nodes.[18] Spatially inhomogeneous DQMoM approaches are more complicated, as they require discretization of spatial derivatives.[18]

The solution techniques of QMoM and DQMoM are only able to solve for the evolution of the mixture as a whole and information on discrete species, such as species vapor molar flow rates and liquid mole fractions, are not calculated by such models.[11,12,13] In order to reconstruct information on the discrete species, a delumping method was developed to capitalize on the fact that the previously non-linear governing ODEs for the vaporizing droplet are linearized once the mixture properties are known from the DQMoM calculation.[14] DQMoM with delumping has been shown to be a computationally efficient and accurate method for obtaining information on all discrete species for a multicomponent droplet model with infinite liquid diffusivity.[14]

Thus far, a major limitation of QMoM and DQMoM approaches has been their exclusive application to well-mixed droplets and it has been questioned[19,20,21,22] whether these methods can be extended to model droplets with finite liquid diffusivity. This limitation has been presented as a significant flaw in the method[20] since the importance of species gradients within the liquid droplet has been discussed extensively.[4,20,21] Therefore, the model developed in this paper addresses the need for computationally efficient moment methods to be expanded to models with finite liquid diffusivity by using a new modeling strategy for droplet vaporization which augments a monovariate homogeneous DQMoM approach by coupling the DQMoM ODEs to additional algebraic moment equations to solve for the evolution of two related distributions.

The computational approach developed in this paper is applied to the quasi-steady portion of the finite diffusivity DCM developed in[3] which solves ODEs and algebraic equations for the evolution of the average and surface liquid mole fractions within the droplet. To complement the models for quasi-steady behavior, transient models utilizing shape factors and higher order polynomials have been presented.[3,23] While the CTM approach developed here could also be extended to these transient portions of the models, there are limitations to delumping these solutions. Therefore, the computational method presented below is applied to the quasi-steady multicomponent droplet vaporization model.

The principle novelty of the method presented here is in the development of a Coupled Algebraic-Direct Quadrature Method of Moments (CA-DQMoM) approach for a vaporizing multicomponent droplet with finite liquid diffusivity. The method solves for two liquid mole fraction distributions, one governed by ODEs and the other by algebraic equations. The method improves accuracy by taking into account finite rates of liquid diffusion within the droplet without requiring the complex discretization of a spatially inhomogeneous DQMoM application. In Section 2, the CA-DQMoM method will be derived. An approximate version which employs the same nodes for both distributions will also be presented which increases computational efficiency but is restricted to certain far-field boundary conditions. A second novelty of the paper is the adaptation of the delumping method[14] to a finite diffusivity model in order to reconstruct all discrete species information for all times. The accuracy and computational efficiency of the CA-DQMoM with delumping approach will be evaluated in Section 3, with conclusions discussed in Section 4.

2. Model development

2.1. Discrete component model (DCM)

Previous DCMs have employed parabolic profiles for temperature[24] and species mass fraction[3] within a multicomponent liquid droplet for Modeling vaporization under quasi-steady behavior. This paper follows a similar approach to derive a DCM on a molar basis for the quasi-steady case. Since the physical aspects of the model presented here are based on the developments of others and the novelty of this paper is in the derivation of the CA-DQMoM with delumping solution method discussed in subsequent sections, only a brief summary of the governing equations is provided below. This DCM will serve as the "exact" model by which to evaluate the accuracy of the delumped CA-DQMoM developed later.

2.1.1. Gas phase equations

Similar to previous works in continuous thermodynamics and droplet vaporization theory,[7,11,12,13,25] the equations for the gas phase are simplified by assuming spherical symmetry, quasi-steady transport for the gas phase, and spatially constant gas phase properties in the boundary layer evaluated using the 1/3 rule.[26] The gas phase transport equation, originally defined on a mass basis,[25] is the classical droplet equation which has been used in molar form in previous moment methods:[11,12,13]

(1)

$$\dot{n}^{tot} = 2\pi R C_g D_g Sh_g^* ln(1 + B_M)$$

where $\dot{n}^{tot}$ is the total vapor molar flow rate. The Spalding transfer number on a molar basis and the modified Sherwood number[25] are defined as

(2)

$$B_M = \frac{x_{g,s}^{tot} - x_{g,\infty}^{tot}}{1 - x_{g,s}^{tot}}$$

(3)

$$Sh_g^* = \frac{2R_f}{R_f - R}$$

where R_f is the limit of the boundary layer. The classical Sherwood number is defined as

(4)

$$Sh_g^i = \frac{2R}{x_{g,\infty}^i - x_{g,s}^i}\left(\frac{\partial x_g^i}{\partial r}\right)_s$$

It is assumed that the diffusion coefficients and Sherwood numbers for each species can be approximated by single averaged values.[11] Thus, the modified Sherwood number can be related to the Sherwood number[25] by the expression

(5)

$$Sh_g^* = \frac{B_M}{ln(1 + B_M)} Sh_g$$

2.1.2. Liquid phase equations

For the liquid phase analysis, the quasi-steady parabolic approach[3] is modified for a molar, rather than mass, basis. It is assumed that the droplet is spherically symmetric, liquid molar concentration changes slowly with time, liquid molar concentration and diffusivity are uniform within the droplet and there is no convection within the droplet. Thus, the species conservation equation can be simplified as

(6)

$$\frac{\partial x_l^i}{\partial t} = \frac{D_l}{r^2}\frac{\partial}{\partial r}\left(r^2 \frac{\partial x_l^i}{\partial r}\right)$$

With the approximation that $\frac{\partial x_l^i}{\partial t}$ is only a function of time,[3] Eq. (6) can be integrated twice to obtain the parabolic profile of the species liquid mole fractions within the droplet:

(7)

$$x_l^i(r,t) = x_{l,c}^i + \left(x_{l,s}^i - x_{l,c}^i\right)\left(\frac{r}{R}\right)^2$$

where r is the radial coordinate, R is the radius of the droplet and the subscripts c and s represent the center and surface of the droplet, respectively. A volume average is performed on Eq. (7) to obtain an expression relating the average, surface, and center liquid mole fractions for each species:

(8)

$$\bar{x}_l^i = \frac{3}{5}x_{l,s}^i + \frac{2}{5}x_{l,c}^i$$

Evaluating the derivative of Eq. (7) at the surface and combining with Eq. (8) results in the expression for the liquid mole fraction gradient for each species at the surface:

(9)
$$\left(\frac{\partial x_l^i}{\partial r}\right)_s = \frac{5}{R}\left(x_{ls}^i - \bar{x}_l^i\right)$$

2.1.3. Governing equations

Similar to the mass based approach,[1,3] species conservation is applied on a molar basis to the interface at the droplet surface:

(10)
$$-C_l\frac{dR}{dt}\left(x_{g,s}^i - x_{l,s}^i\right) + C_l D_l\left(\frac{\partial x_l^i}{\partial r}\right)_s - C_g D_g\left(\frac{\partial x_g^i}{\partial r}\right)_s = 0$$

where the assumptions previously discussed for the liquid and gas phases are applied. Combining Eqs. (4), (5), (9), (10) results in the conservation equation at the interface:

(11)
$$-C_l\frac{dR}{dt}\left(x_{g,s}^i - x_{l,s}^i\right) + \frac{5C_l D_l}{R}\left(x_{ls}^i - \bar{x}_l^i\right) - \frac{C_g D_g Sh_g^* ln(1+B_M)}{2RB_M}\left(x_{g,\infty}^i - x_{g,s}^i\right) = 0$$

Eq. (11) is summed for all discrete species and rearranged to obtain the equation for the rate of surface regression:

(12)
$$\frac{dR}{dt} = -\frac{C_g D_g Sh_g^* ln(1+B_M)}{2C_l R}$$

Species molar conservation is applied to a control volume enclosing the liquid droplet:

(13)
$$\frac{d}{dt}\left(C_l V \bar{x}_l^i\right) = 4\pi R^2\left[C_l D_l\left(\frac{\partial x_l^i}{\partial r}\right)_s + C_l\frac{dR}{dt}x_{l,s}^i\right]$$

Eq. (13) is combined with Eq. (9) and simplified to obtain the ODE for the evolution of the average liquid mole fraction for each species:

(14)
$$\frac{d\bar{x}_l^i}{dt} = \left(\frac{15D_l}{R^2} + \frac{3}{R}\frac{dR}{dt}\right)\left(x_{ls}^i - \bar{x}_l^i\right)$$

As is common in droplet vaporization models,[6,7,11,12,13,16] it is assumed that the mixtures are ideal and therefore, vapor-liquid equilibrium at the droplet surface is established by Raoult's Law:

(15)
$$x_{g,s}^i = x_{l,s}^i\frac{P_{sat}^i(T_{l,s})}{P_\infty}$$

Rearranging Eq. (11) and combining with Eq. (15) results in the algebraic expression for the surface liquid mole fraction of each species:

(16)

$$x_{l,s}^{i} = \frac{5C_l D_l \bar{x}_l^i + \frac{C_g D_g Sh_g^* \ln(1+B_M)}{2B_M} x_{g,\infty}^i}{5C_l D_l + C_l R \frac{dR}{dt}\left(1 - \frac{P_{sat}^i(T_{l,s})}{P_\infty}\right) + \frac{C_g D_g Sh_g^* \ln(1+B_M)}{2B_M} \frac{P_{sat}^i(T_{l,s})}{P_\infty}}$$

Eqs. (14), (16) comprise the system of differential algebraic equations (DAEs) which define the evolution of the droplet composition and are similar to the equations for mass fraction developed in,[3] with the exception that the model presented in this paper accounts for the presence of gaseous fuel at the far-field boundary and assumes constant molar properties as opposed to mass properties.

Although the parabolic model defined in this section is an improvement on the well-mixed model since it takes into account finite liquid diffusion within the droplet, it is not without limitations. As discussed by Sazhin, the accuracy of the parabolic model during initial transience is questionable since it assumes that the parabolic profiles are immediately established.[19,20] It should be noted that the CA-DQMoM approach developed in subsequent sections is not limited to quasi-steady models and could be applied to the transient shape factor DCM.[3] However, it would not be possible to use delumping on the CA-DQMoM solution due to the dependence of the shape factor on the surface liquid mole fraction. Therefore, the derivation of the computational method will focus on the quasi-steady case only.

Similar to the original well-mixed DQMoM with delumping model,[14] the model developed in this paper can be solved with a variety of temperature profile assumptions including uniform, quasi-steady, or effective conductivity models. For the results presented in this paper, the liquid temperature within the droplet was modeled using a parabolic temperature profile[24] with the following equations obtained from Laurent:[16]

(17)

$$\frac{d\bar{T}_l}{dt} = \frac{3}{2} \frac{k_g Nu_g^* \ln(1+B_T)}{C_l c_{p,l} R^2 B_T \left(1 + \frac{1}{10}\left(\frac{k_g Nu_g^* ln(1+B_T)}{k_l B_T}\right)\right)} \left(T_\infty - \frac{B_T l_v}{c_{p,v}} - \bar{T}_l\right)$$

(18)

$$T_{l,s} = \bar{T}_l + \frac{R^2 C_l c_{p,l}}{15 k_l} \frac{d\bar{T}_l}{dt}$$

2.2. Coupled Algebraic-Direct Quadrature Method of Moments (CA-DQMoM)

As previously discussed, QMoM and DQMoM approaches have, thus far, only been applied to well-mixed droplet models and it has been questioned whether they can be applied to less restrictive cases.[19,20,21,22] The model derived here expands the applicability of moment methods to finite diffusivity models by coupling a DQMoM approach with algebraic moment equations. First, the quasi-steady DCM of the previous section is converted to a CTM. The average liquid mole fraction is taken to be a monovariate continuous function of a distribution variable, I,[18] thus giving the continuous form of Eq. (14):

(19)

$$\frac{d\bar{x}_l(I)}{dt} = S(I,t)$$

where the source term for the finite diffusivity model is given by

(20)
$$S(I,t) = \left(\frac{15D_l}{R^2} + \frac{3}{R}\frac{dR}{dt}\right)\left(x_{l,s}(I) - \bar{x}_l(I)\right)$$

For the purposes of this paper, the distribution variable, *I*, is the normal boiling temperature, T_{nb}. In contrast to the well-mixed model, the quasi-steady finite diffusivity DCM contains an additional algebraic relationship for the surface liquid mole fraction, $x_{l,s}$. This algebraic expression, given in Eq. (16), is similarly converted to continuous form:

(21)
$$x_{l,s}(I) = \frac{5C_l D_l \bar{x}_l(I) + \frac{C_g D_g Sh_g^* \ln(1+B_M)}{2B_M} x_{g,\infty}(I)}{5C_l D_l + C_l R\frac{dR}{dt}\left(1 - \frac{P_{sat}(I,T_{l,s})}{P_\infty}\right) + \frac{C_g D_g Sh_g^* \ln(1+B_M)}{2B_M}\frac{P_{sat}(I,T_{l,s})}{P_\infty}}$$

The original well-mixed DQMoM model with a single liquid mole fraction distribution[13] was developed by applying a monovariate, spatially homogenous DQMoM approach.[18] In contrast, the finite diffusivity model requires the solution of two separate liquid mole fraction distributions, one for the average $(\bar{x}_l)$ and one for the surface $(x_{l,s})$, which are related by the algebraic relationship of Eq. (21). Therefore, the finite liquid diffusivity model requires two sets of N weights and two sets of N nodes to be defined. The average weights, $\bar{w}_j$, and average nodes, $\bar{I}_j$, characterize the composition of the droplet with respect to the average liquid mole fraction. The surface weights, $w_{s,j}$, and surface nodes, $I_{s,j}$, similarly correspond to the liquid composition at the droplet surface. The subscript j represents the node index, with j = 1:N, resulting in 4 N unknowns for $\bar{w}_j$, $\bar{I}_j$, $w_{s,j}$, $I_{s,j}$. DQMoM, as developed in,[18] is applied to the average liquid mole fraction distribution since $\bar{x}_l$ is the differential variable. A moment transform is applied to Eq. (19) to obtain 2N ODEs for the evolution of the moments of the average liquid mole fraction distribution:

(22)
$$\frac{d\bar{m}_l^k}{dt} = \bar{S}_k = \int_0^\infty S(I)I^k dI$$

where *k* is the index for the moments and is evaluated for $k = 0{:}\,2N-1$.

In the original well-mixed DQMoM model,[13] the single mole fraction distribution was extracted from the integral in Eq. (22), with the remaining terms being nearly polynomial, in order to apply the Gaussian quadrature approximation.[27] However, for the finite diffusion model, the integral in Eq. (22) must be separated into two integrals so that the average and surface mole fraction distributions can be extracted:

(23)
$$\bar{S}_k = \int_0^\infty S(I)I^k dI = \int_0^\infty x_{l,s}(I)f(I)dI - \int_0^\infty \bar{x}_l(I)f(I)dI$$

where the term $f(I)$ represents the terms left over and is given by

(24)

$$f(I) = \left(\frac{15D_l}{R^2} + \frac{3}{R}\frac{dR}{dt}\right) I^k$$

A Gaussian quadrature approximation is needed for both the average and surface liquid mole fraction distributions. As discussed, each distribution has its own set of weights and nodes:

(25)

$$\int_0^\infty \bar{x}_l(I) f(I) dI \approx \sum_{j=1}^{N} \bar{w}_j f\left(\bar{I}_j\right)$$

(26)

$$\int_0^\infty x_{l,s}(I) f(I) dI \approx \sum_{j=1}^{N} w_{s,j} f\left(I_{s,j}\right)$$

DQMoM solves for the evolution of the weights and nodes of the Gaussian quadrature directly instead of solving for the evolution of the moments, as is done in QMoM.[18,27] Additionally, DQMoM does not require the closure algorithm that QMoM does[18] and has been proven to be more stable for Modeling droplet vaporization.[13] In DQMoM, the distribution function for the differential variable is approximated as the sum of N delta functions, evaluated at the nodes of the distribution variable, multiplied by the weights.[18] Thus, the continuous average liquid mole fraction distribution, $\bar{x}_l(I)$, is set equal to a sum of delta functions evaluated at the average liquid nodes, $\bar{I}_j$, and multiplied by the average liquid weights, $\bar{w}_j$:

(27)

$$\bar{x}_l(I) = \sum_{j=1}^{N} \bar{w}_j \delta\left(I - \bar{I}_j\right)$$

Taking the derivative and combining with Eq. (19) yields

(28)

$$\frac{d\bar{x}_l(I)}{dt} = \sum_{j=1}^{N} \frac{\partial}{\partial t}\left[\bar{w}_j \delta(I - \bar{I}_j)\right] = S(I,t)$$

To develop the DQMoM matrix, the product rule, chain rule, and a moment transform are applied to Eq. (28). Details of the full derivation of the left hand side of the DQMoM matrix can be found in.[13,18] The resulting DQMoM system of equations is given by:

(29)

$$(1-k)\sum_{j=1}^{N} \bar{I}_j^k \frac{d\bar{w}_j}{dt} + k\sum_{j=1}^{N} \bar{I}_j^{k-1} \frac{d(\bar{w}_j \bar{I}_j)}{dt} = \int_0^\infty S(I) I^k dI = \bar{S}_k$$

where the moments are evaluated for $k = 0{:}\,2N-1$.

In matrix form, Eq. (29) is given by

$$\begin{bmatrix} 1 & \cdots & 1 & 0 & \cdots & 0 \\ 0 & \cdots & 0 & 1 & \cdots & 1 \\ -I_1^2 & \cdots & -I_N^2 & 2I_1 & \cdots & 2I_N \\ \vdots & \vdots & \vdots & \vdots & \vdots & \vdots \\ 2(1-N)I_1^{2N-1} & \cdots & 2(1-N)I_N^{2N-1} & (2N-1)I_1^{2N-2} & \cdots & (2N-1)I_N^{2N-2} \end{bmatrix} \times \begin{bmatrix} \dot{w}_1/dt \\ \vdots \\ \dot{w}_N/dt \\ \dot{w}_1 I_1/dt \\ \vdots \\ \dot{w}_N I_N/dt \end{bmatrix} = \begin{bmatrix} \dot{S}_0 \\ \vdots \\ \vdots \\ \vdots \\ \vdots \\ \dot{S}_{2N-1} \end{bmatrix}$$

Although the basic DQMoM approach for the left hand side is the same for both the well-mixed[13] and finite diffusivity models, the right hand side source terms are quite different. To obtain the source terms, $\dot{S}_k$, the Gaussian quadrature approximations of Eqs. (25), (26) are applied to Eq. (23):

(31)

$$\dot{S}_k = \left(\frac{15D_l}{R^2} + \frac{3}{R}\frac{dR}{dt}\right)\left[\sum_{j=1}^{N} w_{s,j} I_{s,j}^k - \sum_{j=1}^{N} \dot{w}_j \dot{I}_j^k\right]$$

The ODEs of Eq. (30) combined with the source terms of Eq. (31) provide 2N equations. For a typical homogeneous DQMoM $I_{s,j}$ approach like that of the original well-mixed DQMoM model,[13] the 2N ODEs would be sufficient to solve for the evolution of the N weights and N nodes of the single distribution. However, for the present model with two distributions and 4N unknowns $\left(\dot{w}_j, \dot{I}_j, w_{s,j}, I_{s,j}\right)$, an additional 2N equations are required to solve for the evolution of the droplet. This is where the coupled algebraic portion of the CA-DQMoM method is needed: an additional 2N algebraic equations are required to simultaneously solve for the algebraic variables $w_{s,j}$ and. These 2N equations are obtained by applying a moment transform and quadrature approximations to the algebraic expression for the continuous surface liquid mole fraction distribution. Applying a moment transform to Eq. (21) and factoring out the original mole fraction distributions results in the following equation:

(32)

$$\int_0^\infty x_{l,s}(I) f_1(I) dI = \int_0^\infty \dot{x}_l(I) f_2(I) dI + \int_0^\infty x_{g,\infty}(I) f_3(I) dI$$

where after some rearrangement, the functions of the terms left over can be written as

(33)

$$f_1(I) = \left[5C_l D_l + C_l R \frac{dR}{dt}\left(1 - \frac{P_{sat}(I,T_{l,s})}{P_\infty}\right) + \frac{C_g D_g Sh_g^* \ln(1+B_M)}{2B_M}\frac{P_{sat}(I,T_{l,s})}{P_\infty}\right] I^k$$

(34)

$$f_2(I) = 5C_l D_l I^k$$

(35)

$$f_3(I) = \frac{C_g D_g Sh_g^* \ln(1+B_M)}{2B_M} I^k$$

An additional quadrature approximation is defined for the far-field gas phase mole fractions

(36)

$$\int_0^\infty x_{g,\infty}(I) f(I) dI \approx \sum_{i=1}^{n} x_{g,\infty}^i f(T_{nb}^i)$$

where the summation is evaluated for the n discrete species since the far-field gas composition is assumed to be constant and known. Thus, applying the quadrature approximations of Eqs. (25), (26), (36) to Eq. (32) results in the 2N coupled algebraic expressions given by

(37)

$$\sum_{j=1}^{N}\left[5C_l D_l + C_l R \frac{dR}{dt}\left(1 - \frac{P_{sat}(I_{s,j},T_{l,s})}{P_\infty}\right) + \frac{C_g D_g Sh_g^* \ln(1+B_M)}{2B_M}\frac{P_{sat}(I_{s,j},T_{l,s})}{P_\infty}\right] w_{s,j} I_{s,j}^k$$

$$= \sum_{j=1}^{N} 5C_l D_l \bar{w}_j \bar{I}_j^k + \sum_{i=1}^{n} \frac{C_g D_g Sh_g^* \ln(1+B_M)}{2B_M} x_{g,\infty}^i T_{nb,i}^k$$

where the moments are evaluated for $k = 0{:}\,2N-1$. Thus, the final CA-DQMoM model consists of the 2 N DQMoM ODEs in Eq. (30) coupled with the 2 N algebraic expressions in Eq. (37) to solve for $\bar{w}_j$, $\bar{I}_j$, $w_{s,j}$, and $I_{s,j}$.

The initial conditions for the differential variables, $\bar{w}_j$ and $\bar{I}_j$, are calculated using QMoM and Wheeler's algorithm,[28] utilizing the same method as the well-mixed model.[14] Since the surface weights and nodes are algebraically calculated variables, the DAE solver computes consistent initial conditions for $w_{s,j}$, and $I_{s,j}$.

2.3. Delumping

Delumping enables the reconstruction of discrete species information following a computationally efficient CTM solution. A delumping method was previously used for algebraic equations to calculate species information from CTMs for flash tank calculations.[29,30] Delumping of a DQMoM solution to the nonlinear differential equations governing droplet vaporization was demonstrated by Singer.[14] At the completion of the CA-DQMoM solution, all of the total mixture properties are known at every time step which linearizes the original non-linear discrete ODE. The now linear first order ODE can then be

easily solved using an integrating factor.[14,31] Because delumping only involves numerical integration, it is very computationally efficient.[14]

The differential equation for the average liquid mole fraction in Eq. (14) cannot be delumped as written since it is dependent on both $\bar{x}_l^i$ and $x_{l,s}^i$. Therefore, for delumping to be applicable, Eq. (14) must be combined with Eqs. (12), (16) and rearranged to obtain an ODE in terms of $\bar{x}_l^i$, the constant boundary conditions, and the total mixture properties:

(38)
$$\frac{d\bar{x}_l^i}{dt} - \frac{(A-C)(CG_i)}{(A-CG_i)}\bar{x}_l^i = \frac{(A-C)(CE_i)}{(A-CG_i)}$$

where the time dependent terms A, C, E_i, and G_i are defined as

(39)
$$A = \frac{15D_l}{R^2}$$

(40)
$$C = \frac{3C_g D_g Sh_g^* \ln(1+B_M)}{2C_l R^2}$$

(41)
$$E_i = \frac{x_{g,\infty}^i}{B_M}$$

(42)
$$G_i = 1 - \frac{P_{sat}^i(T_{l,s})}{P_\infty} - \frac{P_{sat}^i(T_{l,s})}{P_\infty B_M}$$

In each of these terms, the mixture properties are calculated from the results of CA-DQMoM, the values of the far-field gas phase mole fractions, $x_{g,\infty}^i$, are known constants, and the saturation pressure, P_{sat}^i, is only a function of normal boiling temperature, T_{nb}^i, and the liquid surface temperature of the droplet, $T_{l,s}$. Thus, the terms A, C, E_i, and G_i are independent of $\bar{x}_l^i$ and $x_{l,s}^i$ and the ODE is now a linear, first order differential equation. The integrating factor method[31] is used to solve the ODE, with the following integrating factor

(43)
$$u_i(t) = \exp\left[\int_0^t -\frac{(A-C)(CG_i)}{(A-CG_i)}dt\right]$$

Thus, the solution for the average liquid mole fraction for each discrete species at every time is given by

(44)
$$\bar{x}_l^i(t) = \frac{\int_0^t u_i(t)\frac{(A-C)(CE_i)}{(A-CG_i)}dt + \bar{x}_l^i(0)}{u_i(t)}$$

The surface liquid mole fractions can then be calculated explicitly using the algebraic relationship in Eq. (16). Using the same time dependent terms A, C, E_i, and G_i, the equation for the surface liquid mole fraction of each discrete species is given by

(45)

$$x_{l,s}^{i}(t) = \frac{A\bar{x}_{l}^{i}(t) + CE_i}{A - CG_i}$$

Because delumping a CA-DQMoM solution only involves numerically integrating a linear, first order ODE followed by an explicit algebraic equation, it adds great benefit at very little computational expense.

2.4. Other submodels

The property correlations and mixing rules utilized in this paper for kerosene are obtained from,[12,16,32] and are the same as those previously used in DQMoM with delumping for the well-mixed droplet summarized in the Appendix of.[14] The liquid properties for the droplet are calculated using the average nodes, $\bar{I}_j$, and the average liquid temperature, $\bar{T}_l$ while the properties of the gas are calculated using the surface nodes, $I_{s,j}$, and constant far-field boundary conditions following the 1/3 rule.

2.5. CA-DQMoM with node approximation

The system of DAEs developed using the CA-DQMoM approach defined in Section 2.2 is based on two sets of weights and nodes: one set to characterize the average liquid mole fraction distribution and one set to characterize the surface liquid mole fraction distribution. A simplification can be made to this system of equations if it is assumed that a single set of nodes can be used for both distributions, or $\bar{I}_j \approx I_{s,j}$. This approximation is only valid when there is either no condensation on the droplet surface or if the condensate has a similar composition to that of the average liquid droplet composition. In other words, this approximation can be used if the constant far-field gas phase composition ($x_{g,\infty}^{i}$) is either pure air or a percentage of stoichiometric gaseous fuel. Applying the CA-DQMoM with node approximation approach results in a system of only 3 N unknowns $\left(\bar{I}_j, \bar{w}_j, w_{s,j}\right)$ and therefore, Eq. (37) only needs to be solved for $k = 0{:}\, N-1$. Thus, the CA-DQMoM system of DAEs is reduced by N algebraic equations, leading to more computational savings.

The reason that CA-DQMoM with node approximation is only valid for certain boundary conditions is similar to the limitations of CTMs which assume the distribution shape is represented by a gamma function.[11] Constraining the surface distribution to be defined by the average nodes is similar, but not as restrictive, to assigning a fixed shape to the surface distribution. In test cases where the shape of the surface distribution mimics that of the average distribution, the approximation of $\bar{I}_j \approx I_{s,j}$ is valid. However, for atypical condensate compositions, such as a single component of the fuel present at the far-field boundary, the surface distribution will have a shape that is distinct from the average distribution and a full CA-DQMoM solution with $\bar{I}_j \neq I_{s,j}$ must be utilized. The applicability of CA-DQMoM with node approximation and the associated computational savings are demonstrated in Section 3.

2.6. Numerical approach

Similar to the well-mixed model,[14] both the CA-DQMoM model and the finite diffusivity DCM used for comparison were solved in MATLAB utilizing the IDA solver developed by the Lawrence Livermore National Laboratory.[33] Both the CA-DQMoM and the DCM models contain one ODE for temperature, one algebraic temperature equation, and one ODE for droplet radius. While the DCM model for a droplet with n components also solves n species ODEs and n algebraic species equations, the CA-DQMoM model utilizing N nodes solves 2N species ODEs and 2N algebraic species equations. Therefore, the DCM solves 2n + 3 equations while the CA-DQMoM model solves 4N + 3 equations, typically with $N \ll n$. The delumping step, which involves integrals with respect to time, was computed using the trapezoid rule following the CA-DQMoM solution for the time interval.[14] To utilize CA-DQMoM with delumping in a CFD simulation, the delumping step would need to be performed following every time step. A technique requiring only the current and previous time step for the integration as described in[14] would also apply to the finite diffusivity model.

3. Results and discussion

The CA-DQMoM with delumping model for a multi-component droplet with finite liquid diffusivity was validated by comparing the results to those calculated using a DCM, which is considered to be an exact solution with respect to the model derived above. In order to demonstrate the accuracy and computational savings achieved using CA-DQMoM with delumping, test cases were performed for droplets ranging from 36 to 200 components.

3.1. Droplet with 36 species (kerosene)

Test conditions were specified for a 50 µm droplet of kerosene initially at 300 K exposed to gas at 500 K and 5 bar.[12] The far-field conditions are specified as $x_{g,\infty}^{air} = 0.7$ and $x_{g,\infty}^{i=1} = 0.3$ where the first component i = 1 corresponds to isohexane, the most volatile component.[12] As discussed in,[12] these boundary conditions result in a computationally difficult test case for CTM, with condensation initially occurring. Similar to the well-mixed models,[12,13] it is assumed that the boundary conditions are constant. The normal boiling points and initial liquid composition for the 36 species of kerosene are taken from[16] and are used as the initial conditions for the average liquid mole fractions.

CA-DQMoM was applied to the kerosene droplet using N = 2, 3, and 4 nodes. Fig. 1, Fig. 2, Fig. 3 show the evolution of the average and surface weights and nodes for the three cases. Similar to the results of the well-mixed droplet,[13] the CA-DQMoM weights and nodes are smooth and stable.

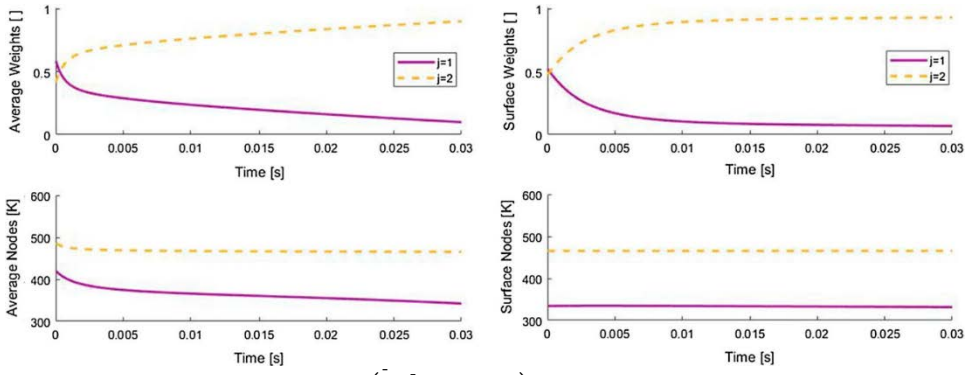

Fig. 1. Evolution of CA-DQMoM weights and nodes $\left(\bar{I}_j, w_j, \bar{I}_{s,j}, w_{s,j}\right)$ for N = 2 for the kerosene test case.

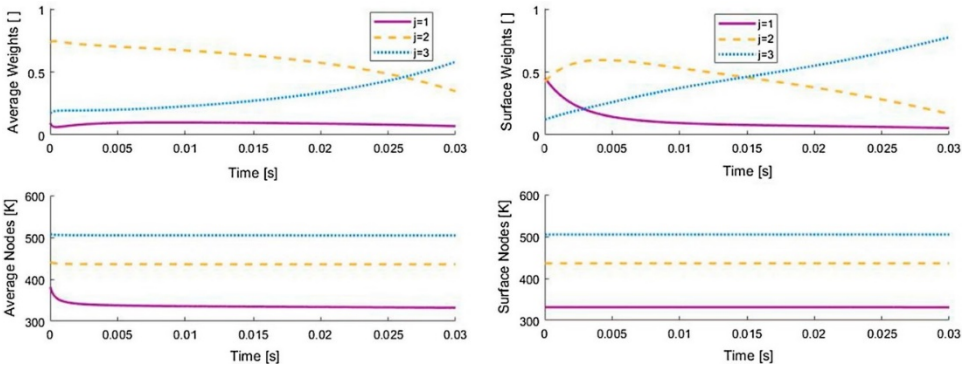

Fig. 2. Evolution of CA-DQMoM weights and nodes $\left(\bar{I}_j, \bar{w}_j, I_{s,j}, w_{s,j}\right)$ for N = 3 for the kerosene test case.

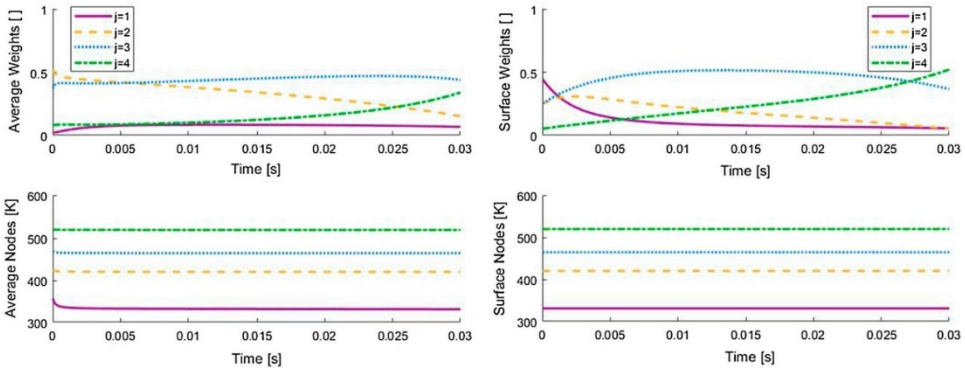

Fig. 3. Evolution of CA-DQMoM weights and nodes $\left(\bar{I}_j, \bar{w}_j, I_{s,j}, w_{s,j}\right)$ for N = 4 for the kerosene test case.

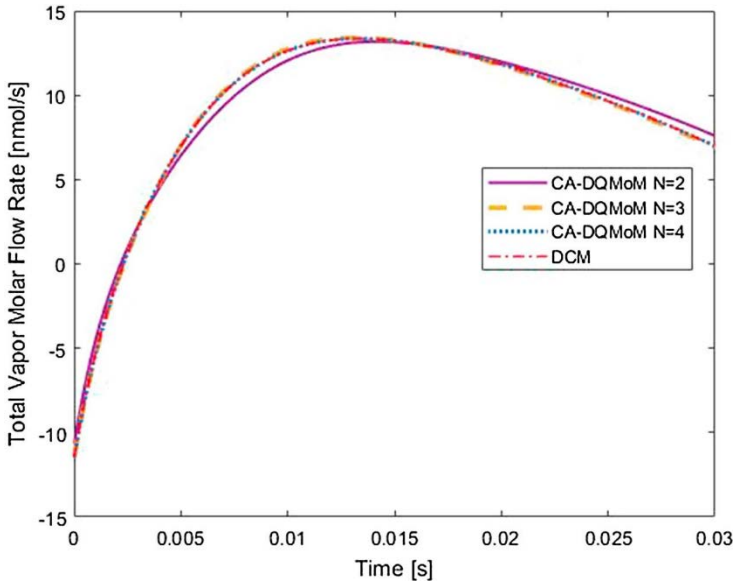

Fig. 4. Evolution of total vapor molar flow rate with time for CA-DQMoM (N = 2, 3, and 4) compared to the DCM for the kerosene test case.

The accuracy of the CA-DQMoM model was first evaluated by comparing the results for the total mixture to those calculated using the DCM. Fig. 4 shows the total vapor molar flow rate calculated with N = 2, 3, and 4 compared to the DCM. CA-DQMoM with N = 3 and 4 produces extremely accurate

results for the evolution of the total mixture, including during initial condensation where the total molar flow rate is negative. There is slight error observed for the total molar flow rate calculated with N = 2.

The delumping portion of the model builds on the CA-DQMoM results and provides information on each real discrete species. The accuracy of CA-DQMoM with delumping (N = 3) is demonstrated in Fig. 5a and b for the average liquid mole fractions and the surface liquid mole fractions, respectively, for each of the 36 components of kerosene at various times. Fig. 6 shows that the vapor molar flow rates for each discrete species, which serve as source terms for the gas-phase solver in CFD codes, are also in good agreement with the values from DCM, including at an early time. The excellent agreement between CA-DQMoM with delumping and DCM affirmatively answers the question[20] of whether moment methods can be successfully extended to droplets with finite liquid diffusivity.

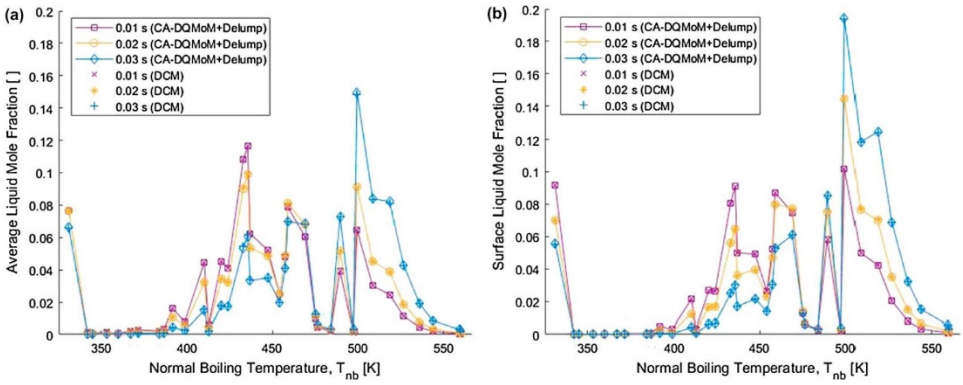

Fig. 5. Comparison of the (a) average and (b) surface liquid mole fraction distributions $\left(\bar{x}_l^i \text{and} x_{l,s}^i\right)$ calculated using CA-DQMoM with delumping (N = 3) and the DCM, at three times for the kerosene test case.

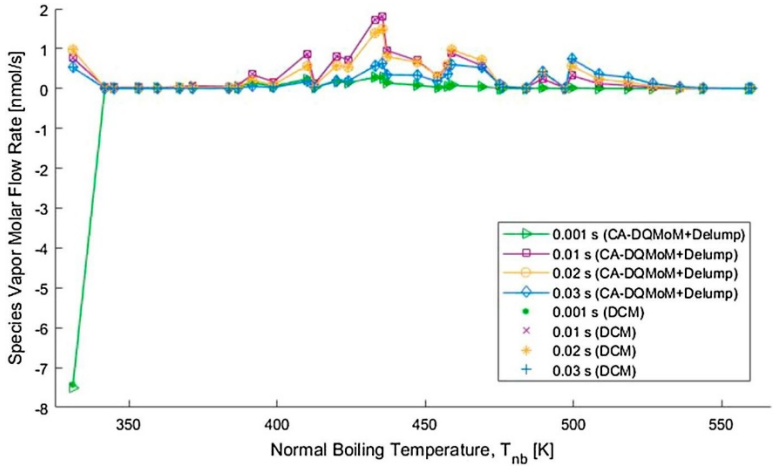

Fig. 6. Comparison of discrete species vapor molar flow rates calculated using CA-DQMoM with delumping (N = 3) and the DCM, at four times for the kerosene test case.

To evaluate the accuracy of CA-DQMoM with delumping as compared to the finite diffusivity DCM, the two-norm relative error was calculated according to the following equation:

(46)

$$err = \frac{\left[\sum_{i=1}^{n}\left(\dot{n}^{i}_{CA-DQMoM} - \dot{n}^{i}_{DCM}\right)^{2}\right]^{1/2}}{\left[\sum_{i=1}^{n}\left(\dot{n}^{i}_{DCM}\right)^{2}\right]^{1/2}}$$

The relative error in species vapor molar flow rates for CA-DQMoM with delumping for N = 2, 3, and 4 compared to the DCM are plotted in Fig. 7 for all times. The relative error decreases significantly from N = 2 to N = 3 with only a slight additional drop in error by increasing the number of CA-DQMoM nodes to N = 4. For N = 3 and N = 4, the relative error is below 1.5% for the majority of the simulation with a brief spike in error during the transition from condensation to evaporation. Based on computation time and accuracy, CA-DQMoM with three nodes would be the best option for implementation into CFD simulations.

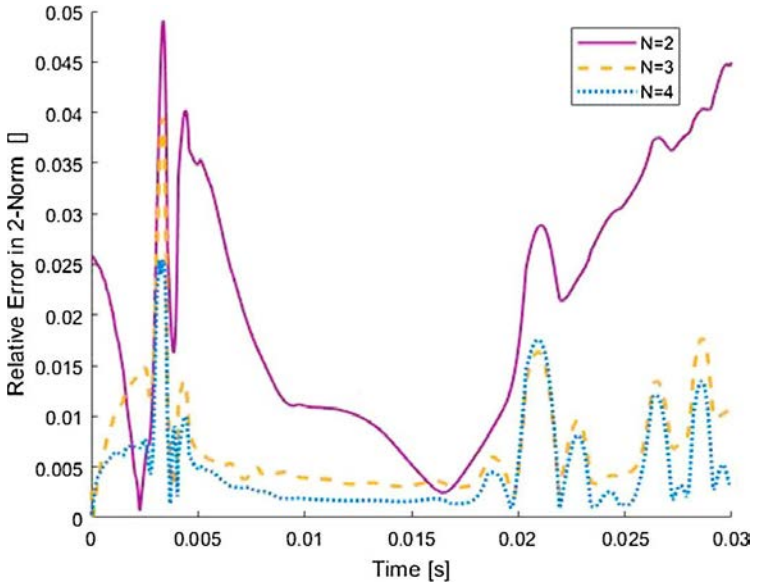

Fig. 7. Two-norm relative error in discrete species vapor molar flow rates calculated using CA-DQMoM with delumping for the kerosene test case.

3.2. Droplet with 200 species

The CA-DQMoM with delumping model was also applied to a droplet composed of 200 hypothetical species. Similar to the first test case, a 50 µm diameter droplet initially at 300 K exposed to gas at 500 K and 5 bar is employed. The initial conditions for the liquid include 200 discrete species with normal boiling points between 331 K and 560 K. The initial average liquid mole fractions are random and are shown in Fig. 8a. The constant far-field gas phase mole fractions, shown in Fig. 8b, are also randomized with a total gaseous fuel composition of 5% and the remaining 95% being air.

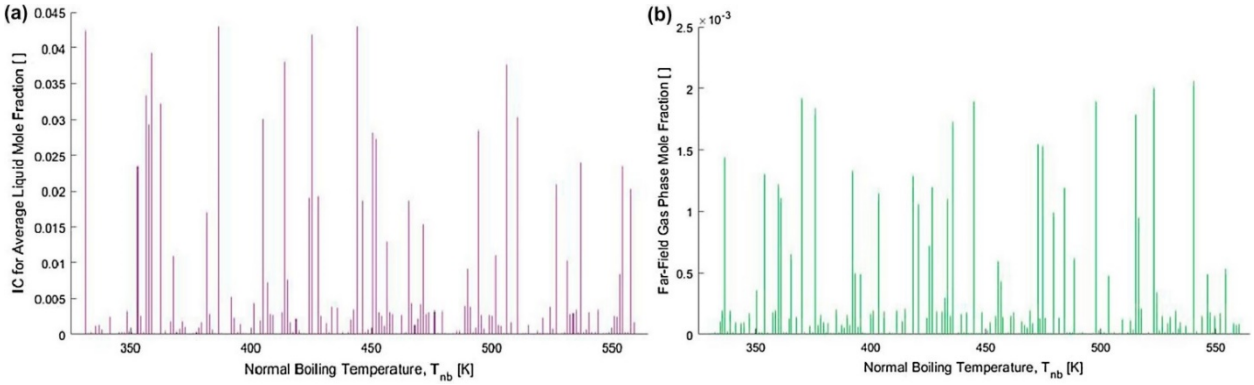

Fig. 8. (a) Initial conditions for the average liquid mole fraction distribution for a droplet with 200 hypothetical species and (b) constant far-field gas mole fraction distribution.

The CA-DQMoM results for droplet radius calculated using N = 2, 3, and 4 are shown in Fig. 9. Similar to the kerosene test case, the total mixture results are extremely accurate for CA-DQMoM with three and four nodes, with a slight error observed for N = 2.

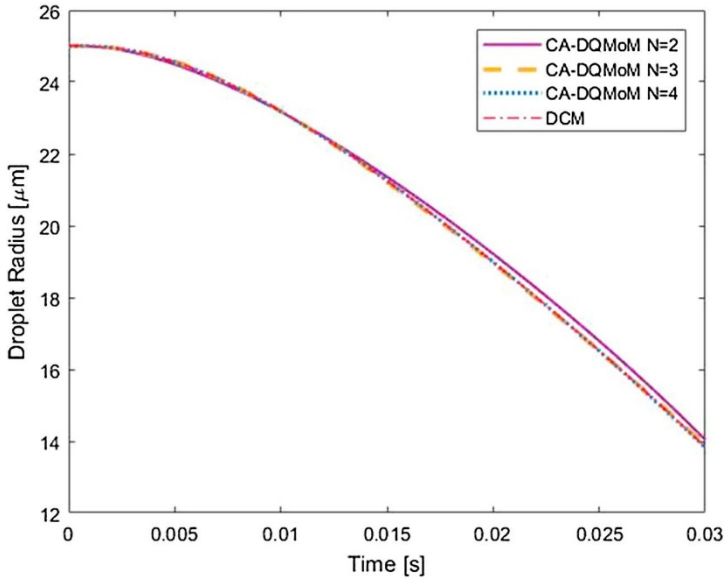

Fig. 9. Evolution of droplet radius with time for CA-DQMoM (N = 2, 3, and 4) compared to the DCM for the 200 species test case.

Delumping was performed following the CA-DQMoM solution and the discrete species results for the 200 hypothetical droplet components were compared to the full DCM. The agreement between the two models is excellent, as shown by the results for species vapor molar flow rates in Fig. 10. The two-norm relative error, defined in Eq. (46), was calculated for the 200 species vapor molar flow rates and is graphed in Fig. 11.

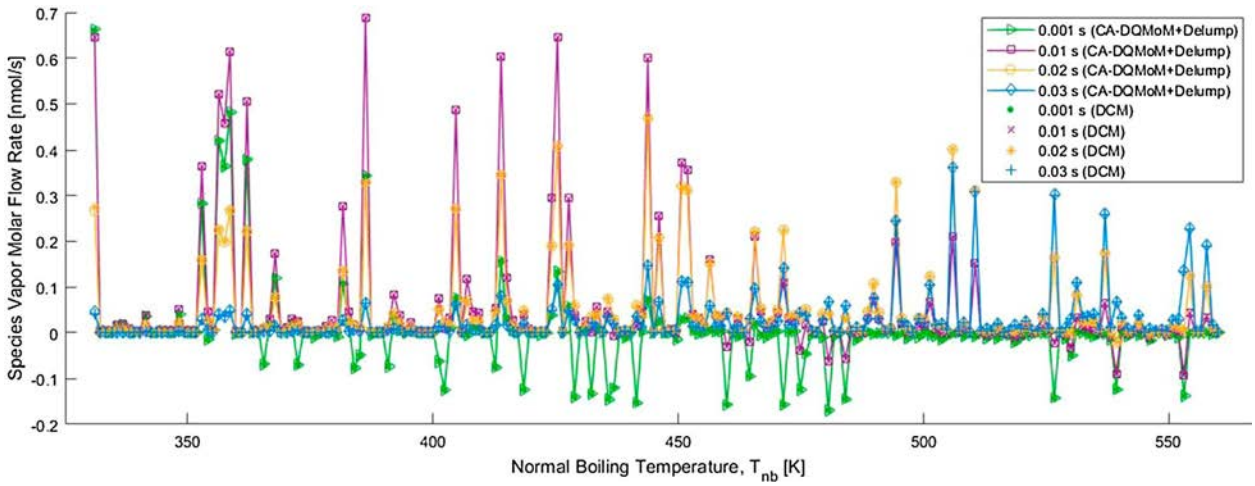

Fig. 10. Comparison of discrete species vapor molar flow rates calculated using CA-DQMoM with delumping (N = 3) and the DCM, at four times for the 200 species test case.

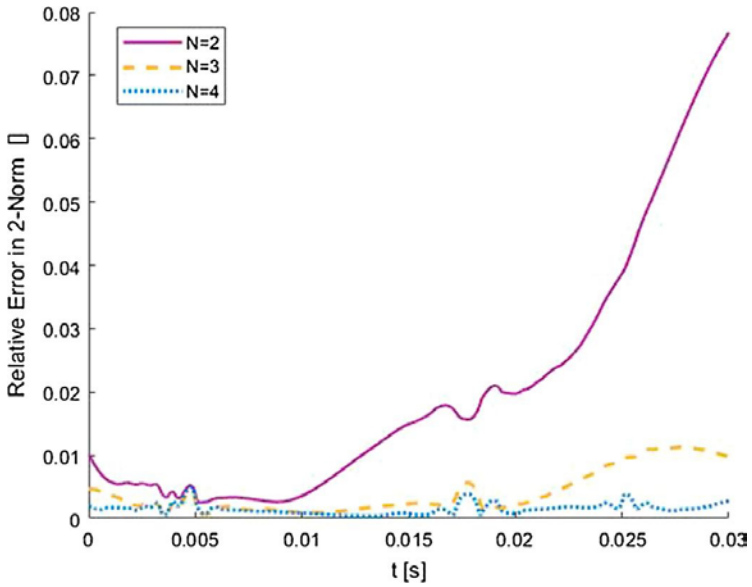

Fig. 11. Two-norm relative error in discrete species vapor molar flow rates calculated using CA-DQMoM with delumping for the 200 species test case.

The advantage of CA-DQMoM with delumping is the reduced computational time compared to a full DCM, without the loss of information on any discrete species. Fig. 12 shows the computational time for various models and numbers of species. For the test case in Section 3.1 with 36 components, CA-DQMoM (N = 3) with delumping is 35% more efficient than the DCM for the finite diffusivity model. As the number of species increases, the computational savings increases greatly, with savings of 62%, 80%, and 92% for 50, 100, and 200 species, respectively, using N = 3. The additional computational time required to perform delumping after a CTM solution is negligible, making it a very attractive method to solve for information on the discrete species.

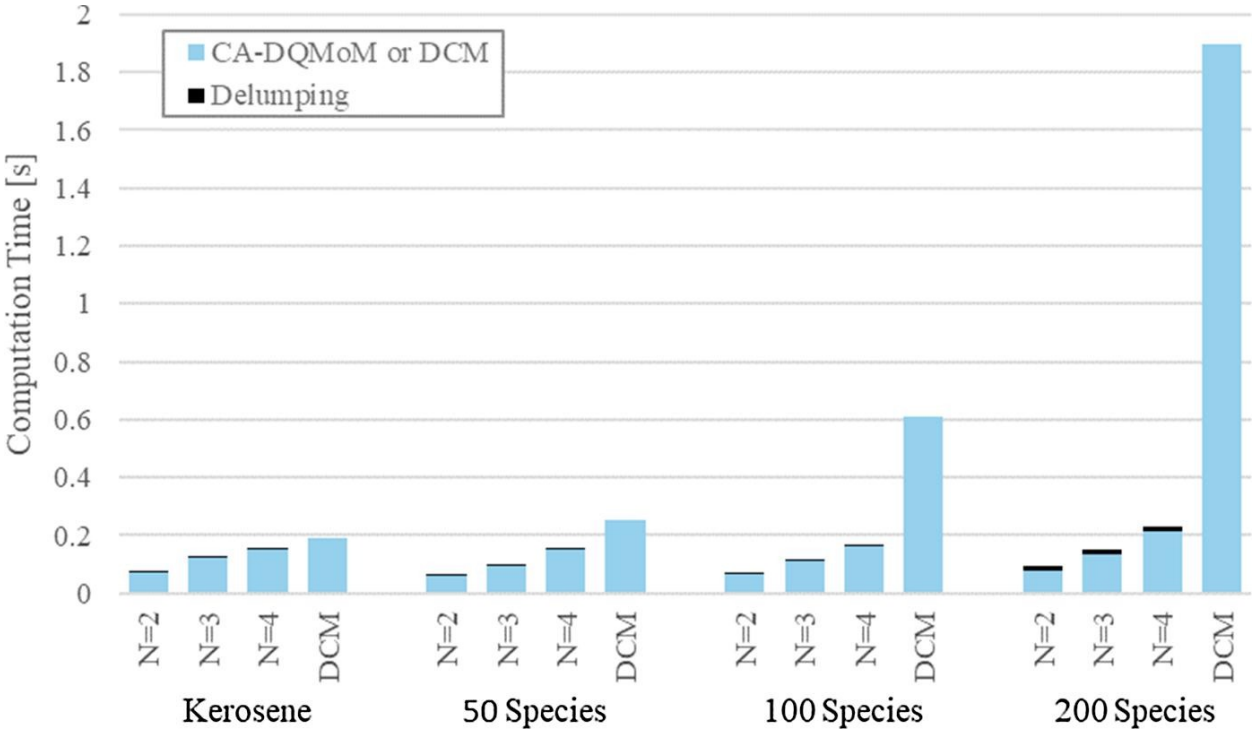

Fig. 12. Comparison of computation times for CA-DQMoM with delumping and DCM for various number of species.

3.3. CA-DQMoM with node approximation

CA-DQMoM with node approximation, as described in Section 2.5, decreases the DAE system by N algebraic equations but is only valid when the boundary conditions are either pure air or a percentage of stoichiometric gaseous fuel. Fig. 13 graphs the total vapor molar flow rates calculated by CA-DQMoM with node approximation, CA-DQMoM, and the DCM for three different boundary conditions for a vaporizing kerosene droplet. The first and second graphs of Fig. 13 show the accuracy of the node approximation model when the boundary conditions are pure air or 30% stoichiometric kerosene gas. The third graph of Fig. 13 shows that for the unique boundary condition of 30% isohexane, which is the most volatile component of the droplet, the approximation of $I_j \approx I_{s,j}$ is not valid and a full DQMoM model with 4N species equations must be used.

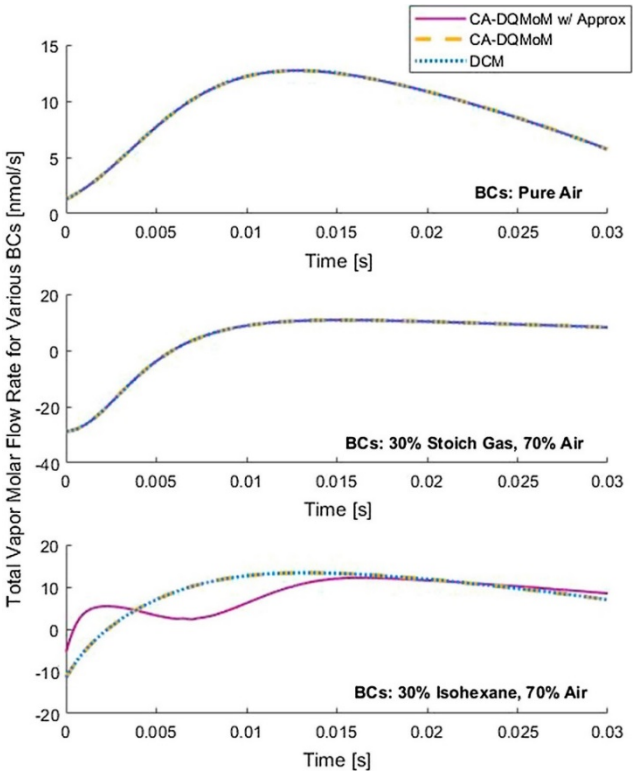

Fig. 13. Evolution of total vapor molar flow rate with time for CA-DQMoM with node approximation (N = 4), CA-DQMoM (N = 4), and DCM for various boundary conditions.

The same delumping procedure can be applied to the node approximation model. The species vapor molar flow rates for the test case of kerosene with pure air at the far-field boundary calculated by node approximation with delumping is compared to the results of the DCM in Fig. 14. Like the CA-DQMoM model, the delumped solution of the CA-DQMoM with node approximation shows excellent agreement with the DCM.

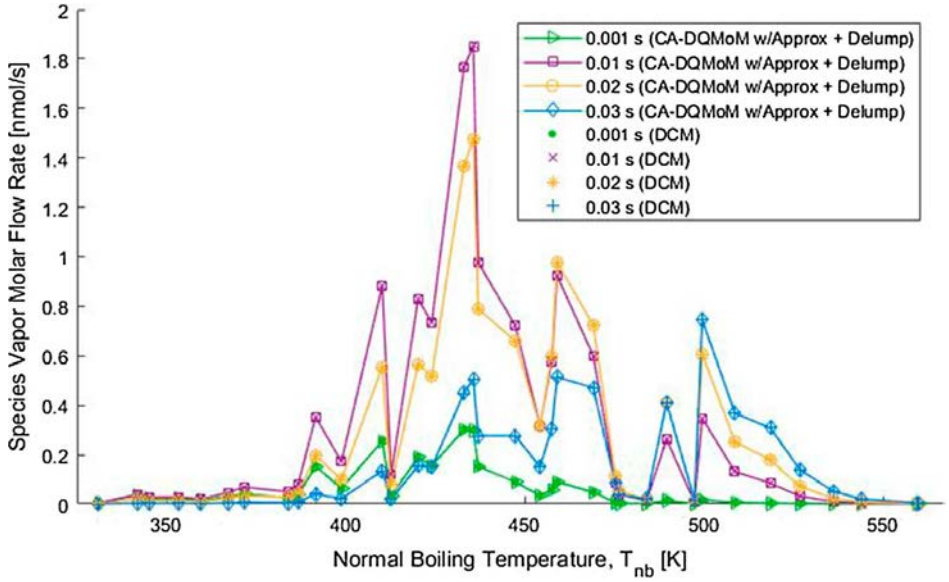

Fig. 14. Comparison of discrete species vapor molar flow rates calculated using CA-DQMoM with node approximation and delumping (N = 3) and the DCM, at four times.

The computational savings achieved by making the node approximation is shown in Fig. 15 for the 36 species kerosene model with a far-field gas composition of pure air. The node approximation eliminates N algebraic equations which results in a computational savings of about 30% for N = 3 and 32% for N = 4.

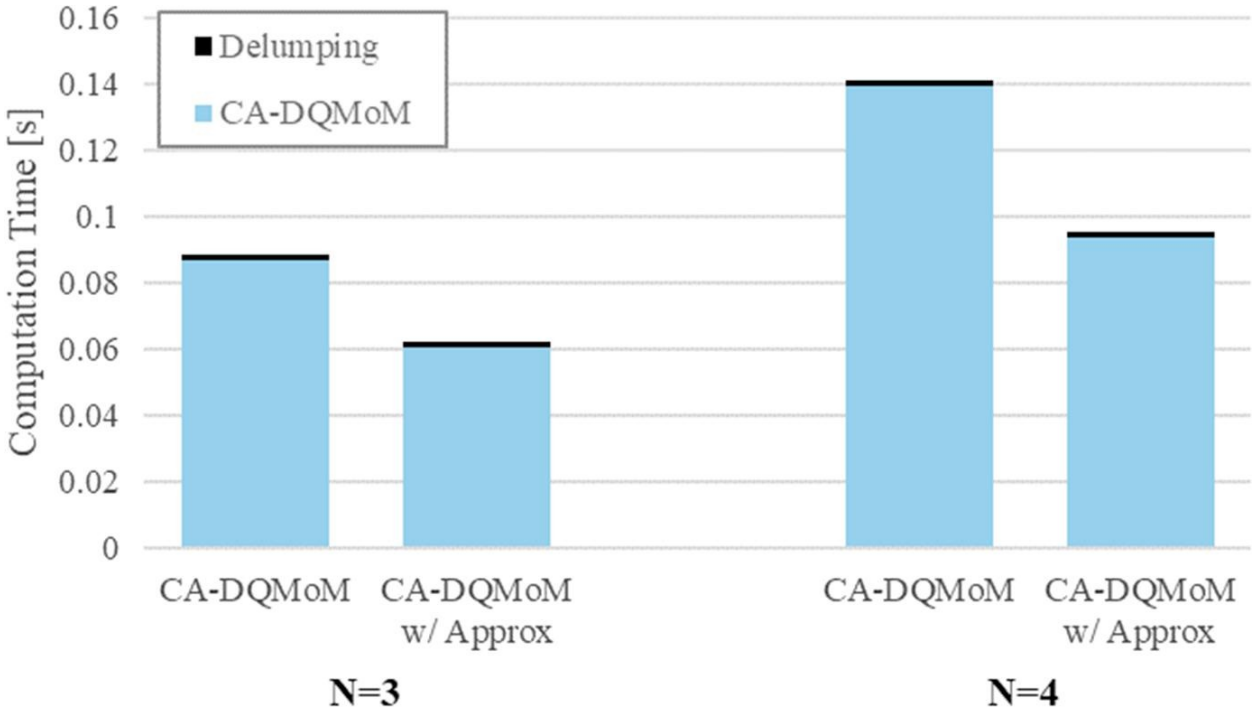

Fig. 15. Comparison of computation times for CA-DQMoM with delumping vs CA-DQMoM with node approximation and delumping for a kerosene droplet vaporizing in pure air.

4. Conclusions

A Coupled Algebraic-Direct Quadrature Method of Moments (CA-DQMoM) with delumping approach has been developed and applied to a vaporizing multicomponent droplet with finite liquid diffusivity. The model differs from previous QMoM and DQMoM approaches[11,12,13,14] by employing two liquid distribution functions in order to account for liquid diffusion within the droplet represented by parabolic liquid mole fraction profiles. The CA-DQMoM model generates a system of DAEs comprised of 2N ODEs and 2N algebraic equations to solve for two sets of CA-DQMoM weights and nodes. After the CA-DQMoM solution, an inexpensive delumping technique[14] was adapted for the finite diffusivity model in order to reconstruct the discrete species information. A supplemental node approximation model was also presented which simplified the CA-DQMoM model for increased computational efficiency and was shown to be appropriate for far-field boundary conditions of pure air or a percentage of stoichiometric gaseous fuel.

The CA-DQMoM model was validated by comparing the delumped results with those of a finite diffusivity DCM. The accuracy of the method was shown to be excellent utilizing N = 3 nodes for any number of discrete species between 36 and 200, with increased accuracy using N = 4 nodes. The computationally difficult case studied by Laurent et al. for a kerosene droplet vaporizing in 30% isohexane gas[12] was solved using CA-DQMoM with delumping, showing the robustness of the solution technique. The most important feature of the model was the minimal computation time required to obtain accurate information on all discrete species. The computational savings for droplets between 36

and 200 species was significant using CA-DQMoM (N = 3) with delumping compared to traditional DCM, with a computational savings of 92% for 200 species.

The CA-DQMoM with delumping approach developed in this paper successfully extends continuous thermodynamics theory to droplets with finite liquid diffusion. The accuracy and computational efficiency achieved by this model, despite the added complexity of finite liquid diffusion, makes it well suited for implementation in combustion CFD simulations.

Acknowledgements

Funding from Marquette University's College of Engineering Legacy Initiative Seed Grant Program is gratefully acknowledged.

[1]D.J. Torres, P.J. O'Rourke, A.A. Amsden. A discrete multicomponent fuel model. *At Sprays*, 13 (2003), pp. 131-172, 10.1615/AtomizSpr.v13.i23.10

[2]Y. Ra, R.D. Reitz. A vaporization model for discrete multi-component fuel sprays. *Int J Multiph Flow*, 35 (2009), pp. 101-117, 10.1016/j.ijmultiphaseflow.2008.10.006

[3]G.J. Brereton. A discrete multicomponent temperature-dependent model for the evaporation of spherical droplets. *Int J Heat Mass Transf*, 60 (2013), pp. 512-522, 10.1016/j.ijheatmasstransfer.2013.01.037

[4]S.S. Sazhin, A.E. Elwardany, E.M. Sazhina, M.R. Heikal. A quasi-discrete model for heating and evaporation of complex multicomponent hydrocarbon fuel droplets. *Int J Heat Mass Transf*, 54 (2011), pp. 4325-4332, 10.1016/j.ijheatmasstransfer.2011.05.012

[5]S.S. Sazhin, M. Al Qubeissi, R. Nasiri, V.M. Gun'ko, A.E. Elwardany, F. Lemoine, et al. A multi-dimensional quasi-discrete model for the analysis of Diesel fuel droplet heating and evaporation. *Fuel*, 129 (2014), pp. 238-266, 10.1016/j.fuel.2014.03.028

[6]J. Tamim, W.L.H. Hallett. A continuous thermodynamics model for multicomponent droplet vaporization. *Chem Eng Sci*, 50 (1995), pp. 2933-2942, 10.1016/0009-2509(95)00131-N

[7]W.L.H. Hallett. A simple model for the vaporization of droplets with large numbers of components. *Combust Flame*, 121 (2000), pp. 334-344, 10.1016/S0010-2180(99)00144-3

[8]Wang D, Lee CF. Continuous thermodynamics finite diffusion model for multicomponent fuel spray evaporation. In: 13th Int. Multidimens. Engine Model. User's Gr. Meet., 2003.

[9]K.G. Harstad, P.C. Le Clercq, J. Bellan. Statistical model of multicomponent-fuel drop evaporation for many-drop flow simulations. *AIAA*, 41 (2003), pp. 1858-1874.

[10]K. Harstad, J. Bellan. Modeling evaporation of Jet A, JP-7, and RP-1 drops at 1 to 15 bars. Combust *Flame*, 137 (2004), pp. 163-177, 10.1016/j.combustflame.2004.01.012

[11]C. Laurent, G. Lavergne, P. Villedieu. Continuous thermodynamics for droplet vaporization: Comparison between Gamma-PDF model and QMoM. *Comptes Rendus Mécanique*, 337 (2009), pp. 449-457, 10.1016/j.crme.2009.06.004

[12]C. Laurent, G. Lavergne, P. Villedieu. Quadrature method of moments for modeling multi-component spray vaporization. *Int J Multiph Flow*, 36 (2010), pp. 51-59, 10.1016/j.ijmultiphaseflow.2009.08.005

[13]Bruyat A, Laurent C, Rouzaud O. Direct Quadrature Method of Moments for Multicomponent Droplet Spray Vaporization. In: 7th Int. Conf. Multiph. Flow, 2010.

[14]S.L. Singer. Direct Quadrature Method of Moments with Delumping for Modeling Multicomponent Droplet Vaporization. *Int J Heat Mass Transf*, 103 (2016), pp. 940-954.

[15]P.L.C. Lage. The quadrature method of moments for continuous thermodynamics. *Comput Chem Eng*, 31 (2007), pp. 782-799, 10.1016/j.compchemeng.2006.08.005

[16]C. Laurent. *Développement et validation de modèles d'évaporation multi-composant.* Ph.D. Thesis Universite de Toulouse, l'Institut Supérieur de l'Aéronautique et de l'Espace (2008).
[17]S. Tonini, G.E. Cossali. On molar- and mass-based approaches to single component drop evaporation modelling. *Int Commun Heat Mass Transf*, 77 (2016), pp. 87-93, 10.1016/j.icheatmasstransfer.2016.06.014
[18]D.L. Marchisio, R.O. Fox. Solution of population balance equations using the direct quadrature method of moments. *J Aerosol Sci, 36* (2005), pp. 43-73, 10.1016/j.jaerosci.2004.07.009
[19]S. Sazhin. *Droplets and sprays*. Springer-Verlag, London (2014), 10.1007/978-1-4471-6386-2
[20]S.S. Sazhin. Modelling of droplet heating and evaporation: recent results and unsolved problems. *Fuel*, 196 (2017), pp. 69-101, 10.1016/j.fuel.2017.01.048
[21]A.E. Elwardany, S.S. Sazhin, A. Farooq. Modelling of heating and evaporation of gasoline fuel droplets: A comparative analysis of approximations. *Fuel*, 111 (2013), pp. 643-647, 10.1016/j.fuel.2013.03.030
[22]M. Al Qubeissi, S.S. Sazhin, J. Turner, S. Begg, C. Crua, M.R. Heikal. Modelling of gasoline fuel droplets heating and evaporation. *Fuel*, 159 (2015), pp. 373-384, 10.1016/j.fuel.2015.06.028
[23]A.Y. Snegirev. Transient temperature gradient in a single-component vaporizing droplet. *Int J Heat Mass Transf*, 65 (2013), pp. 80-94 doi: 10.1016/j.ijheatmasstransfer.2013.05.064
[24]L.A. Dombrovsky, S.S. Sazhin. A simplified non-isothermal model for droplet heating and evaporation. *Int Commun Heat Mass Transf*, 30 (2003), pp. 787-796, 10.1016/S0735-1933(03)00126-X
[25]B. Abramzon, W.A. Sirignano. Droplet vaporization model for spray combustion calculations. *Int J Heat Mass Transf*, 32 (1989), pp. 1605-1618, 10.1016/0017-9310(89)90043-4
[26]G.L. Hubbard, V.E. Denny, A.F. Mills. Droplet evaporation: effects of transients and variable properties. *Int J Heat Mass Transf*, 18 (1975), pp. 1003-1008.
[27]D.L. Marchisio, R.O. Fox. *Multiphase reacting flows: modelling and simulation*. Springer Wien, New York (2007).
[28]J.C. Wheeler. Modified moments and gaussian quadratures. *Rocky Mt J Math*, 4 (1974), pp. 287-296, 10.1216/RMJ-1974-4-2-287
[29]D.V. Nichita, C.F. Leibovici. An analytical consistent pseudo-component delumping procedure for equations of state with non-zero binary interaction parameters. *Fluid Phase Equilib*, 245 (2006), pp. 71-82, 10.1016/j.fluid.2006.03.016
[30]M. Petitfrere, D.V. Nichita, F. Montel. Multiphase equilibrium calculations using the semi-continuous thermodynamics of hydrocarbon mixtures. Fluid Phase Equilib, 362 (2014), pp. 365-378, 10.1016/j.fluid.2013.10.056
[31]C.H. Edwards, D.E. Penney. *Differential equations and boundary value problems* (2nd ed.), Prentice-Hall, Upper Saddle River, New Jersey (2000).
[32]N. Doué. *Modélisation de l'évaporation de gouttes multi-composants*. Ph.D. Thesis L'École Nationale Supérieure (2005)
[33]A.C. Hindmarsh, P.N. Brown, K.E. Grant, S.L. Lee, R. Serban, D.E. Shumaker, et al. SUNDIALS: suite of nonlinear and differential/algebraic equation solvers. *ACM Trans Math Softw*, 31 (2005), pp. 363-396, 10.1145/1089014.1089020